Computer Methods and Programs in Biomedicine 250 (2024) 108197

Contents lists available at ScienceDirect

Computer Methods and Programs in Biomedicine

journal homepage: https://www.sciencedirect.com/journal/computer-methods-and-programs-in-biomedicine

Exploring the disruptions of the neurophysiological organization in Alzheimer's disease: An integrative approach

Víctor Gutiérrez-de Pablo [a,b,*], Jesús Poza [a,b,c], Aarón Maturana-Candelas [a,b], Víctor Rodríguez-González [a,b], Miguel Ángel Tola-Arribas [b,d], Mónica Cano [e], Hideyuki Hoshi [f], Yoshihito Shigihara [f], Roberto Hornero [a,b,c], Carlos Gómez [a,b]

[a] Biomedical Engineering Group, University of Valladolid, Valladolid, Spain
[b] CIBER-BBN, Centro de Investigación Biomédica en Red - Bioingeniería, Biomateriales y Nanomedicina, Spain
[c] IMUVA, Instituto de Investigación en Matemáticas, University of Valladolid, Spain
[d] Department of Neurology, Río Hortega University Hospital, Valladolid, Spain
[e] Department of Clinical Neurophysiology, Río Hortega University Hospital, Valladolid, Spain
[f] Precision Medicine Centre, Hokuto Hospital, Obihiro, Japan

ARTICLE INFO

Keywords:
Dementia due to Alzheimer's disease
Magnetoencephalography
Electroencephalography
Neurophysiological organization
Association network
Network analysis

ABSTRACT

***Background and Objective*:** Alzheimer's disease (AD) is a neurological disorder that impairs brain functions associated with cognition, memory, and behavior. Noninvasive neurophysiological techniques like magnetoencephalography (MEG) and electroencephalography (EEG) have shown promise in reflecting brain changes related to AD. These techniques are usually assessed at two levels: local activation (spectral, nonlinear, and dynamic properties) and global synchronization (functional connectivity, frequency-dependent network, and multiplex network organization characteristics). Nonetheless, the understanding of the organization formed by the existing relationships between these levels, henceforth named neurophysiological organization, remains unexplored. This work aims to assess the alterations AD causes in the resting-state neurophysiological organization.

***Methods*:** To that end, three datasets from healthy controls (HC) and patients with dementia due to AD were considered: MEG database (55 HC and 87 patients with AD), EEG1 database (51 HC and 100 patients with AD), and EEG2 database (45 HC and 82 patients with AD). To explore the alterations induced by AD in the relationships between several features extracted from M/EEG data, association networks (ANs) were computed. ANs are graphs, useful to quantify and visualize the intricate relationships between multiple features.

***Results*:** Our results suggested a disruption in the neurophysiological organization of patients with AD, exhibiting a greater inclination towards the local activation level; and a significant decrease in the complexity and diversity of the ANs (p-value < 0.05, Mann–Whitney U-test, Bonferroni correction). This effect might be due to a shift of the neurophysiological organization towards more regular configurations, which may increase its vulnerability. Moreover, our findings support the crucial role played by the local activation level in maintaining the stability of the neurophysiological organization. Classification performance exhibited accuracy values of 83.91%, 73.68%, and 72.65% for MEG, EEG1, and EEG2 databases, respectively.

***Conclusion*:** This study introduces a novel, valuable methodology able to integrate parameters characterize different properties of the brain activity and to explore the intricate organization of the neurophysiological organization at different levels. It was noted that AD increases susceptibility to changes in functional neural organization, suggesting a greater ease in the development of severe impairments. Therefore, ANs could facilitate a deeper comprehension of the complex interactions in brain function from a global standpoint.

1. Introduction

Alzheimer's disease (AD) is a neurodegenerative disorder, characterized by a progressive cognitive, functional, and behavioral decline. It is the most frequent cause of dementia worldwide, and it is estimated that more than 50 million people suffer from dementia nowadays [1]. Moreover, this number is expected to increase to over 150 million in 2050 [1,2]. This increase in cases is explained by the global population

* Corresponding author at: Biomedical Engineering Group, University of Valladolid, Valladolid, Spain.
E-mail address: victor.gutierrez@gib.tel.uva.es (V. Gutiérrez-de Pablo).

https://doi.org/10.1016/j.cmpb.2024.108197
Received 25 June 2023; Received in revised form 20 December 2023; Accepted 21 April 2024
Available online 24 April 2024

aging, as age is the main risk factor for developing AD [3]. Besides, its economical impact worldwide was estimated to be $1.3 trillion in 2019, and it is expected to be doubled in 2030 [2].

In order to characterize the anomalies in brain function typical of AD, different imaging techniques have been used. Among them, electrophysiological imaging approaches allow to inspect changes in neural oscillatory activity, which are generated by synchronized neuronal activation located in the brain cortex [4,5]. In this regard, the analysis of magnetoencephalography (MEG) and electroencephalography (EEG) activity has been widely employed in the last decades to study the disruptions of these dynamics in neurodegenerative states [6,7]. The high temporal resolution of both techniques allows an accurate tracking of the fast brain oscillations, providing information on the brain activity dynamics and their susceptibility to disruption by the disease [4,8]. Although the neural generators of both MEG and EEG (M/EEG) are similar, they are not exactly equivalent: MEG is generated by intracellular currents, whereas EEG is generated by extracellular ones [9]. Besides, these techniques present different characteristics, regarding spatial resolution, signal-to-noise ratio, and volume conduction effects influence [9].

One of the most illustrative changes associated with AD in M/EEG signals is the slowing of neural activity. M/EEG spectral components were found to shift towards lower frequency bands [10,11], which can be quantified by different spectral parameters [12]. Moreover, using nonlinear measures, a loss of complexity and irregularity of brain oscillations has been observed [13–15]. Dynamical properties of M/EEG activity have also been assessed by means of different metrics, such as Hjorth parameters and different order moments [16–18]. All these spectral, nonlinear, and dynamical features are computed from the M/EEG signals recorded at individual sensors (*i.e.*, local activation level).

To analyze the interactions between multiple brain regions, a substantial amount of research has focused on examining global synchronization of brain activity, which evaluates the functional association between two or more brain regions [4,19]. Functional connectivity (FC) approaches have revealed that AD is associated with increased connectivity in low frequency bands and decreased connectivity in high frequency bands [20,21]. Network science offers a mathematical framework to study the organization of these connections, namely functional network, which has been shown to be altered in AD [22–24]. Additionally, multiplex network organization properties of the cerebral network can be analyzed as another branch of global synchronization, which integrates the interrelationship between functional networks at different frequency bands [25,26]. FC, frequency-dependent network, and multiplex network organization metrics assess the degree of synchronization or coupling between brain regions (*i.e.*, global synchronization level).

As previously mentioned, existing literature demonstrates the impact of AD in individual neurophysiological features and the potential of M/EEG-based analyses to characterize AD disruption [12,14,17,20,24,26]. However, AD is a complex neurological disease, in which isolated approaches are probably not enough to understand its intricate neurophysiological fingerprint. Thus, the analysis of brain activity integrating multiple features derived from neural activity may provide new information about the effect of AD in brain dysfunction. The features that build local activation and global synchronization levels have been studied separately in previous research works [10,12,14,17,20,27]. However, in this study we propose a novel methodology to integrate these parameters in a single, cohesive, holistic framework that is able to display global and intricate associations in the map of existing relationships between functional neural organization, henceforth called the neurophysiological organization. To the best of our knowledge, this is the first time that ANs have been employed to provide a novel perspective of functional neural organization, allowing the assessment of brain disruption in AD from a global picture and revealing new insights into how these levels relate between each other [28,29]. In addition, using three databases containing information on both M/EEG signals provides substantial robustness to the study, allowing for the evaluation of outcome replicability to address the existing scientific crisis [30].

In light of this, we hypothesize that AD alters the neurophysiological organization, leading to changes in the patterns of relationships; these alterations can be assessed using our novel integrative approach. This would enable the characterization of neurodegenerative states with a high level of detail. Therefore, the study objectives are twofold: Firstly, to present an innovative approach for evaluating and quantifying the underlying neurophysiological organization of the resting-state neural activity, and secondly, to investigate the impact of alterations from both a global and a level-based standpoint in AD.

2. Materials and methods

In the present study, we introduce a novel methodology based on ANs to integrate a great amount of information and quantify the intricate structure of interactions associated with neural activity. Particularly, ANs provide a new and scalable framework from network theory, useful to understand the complex relationships between different properties derived from brain activity, characterized by diverse parameters that have been typically analyzed individually [12,14,17,20,26,31,32]. To the best of our knowledge, this is the first study that simultaneously considers all the signal processing methods that have been employed in previous works. Furthermore, the present research involves three databases to assess the replicability and consistency of the results, even considering different neurophysiological techniques (*i.e.*, EEG and MEG).

The workflow of the study was split into three steps which are described in the following sections and summarized in Fig. 1. Firstly **(1)**, the levels of analysis (local activation and global synchronization) were characterized by computing different sublevels of features (spectral, nonlinear, and dynamic features; and FC, frequency-dependent network, and multiplex network organization characteristics) from the M/EEG data. Then **(2)**, association networks (ANs) were generated by means of 50 bootstrap iterations. To minimize the sample size effect on the results, 45 participants were randomly selected on each bootstrap iteration, as 45 is the number of participants in the smallest group of all databases included in the study. ANs summarize the relationships between all the previous parameters, providing the map of relationships which is called "neurophysiological organization". In order to compute the relationships between M/EEG parameters, Spearman's partial correlation coefficient, corrected by age and sex, was calculated. Finally, once all relationships were computed, a threshold of 0.8 was set to solely show 0.8 to 1 absolute correlation values. Afterwards **(3a)**, different network parameters were computed to characterize the ANs alterations caused by the disease (i.e., segregation, integration, centrality, modularity, diversity, and complexity) [19,33,34]. Next **(3b)**, the radii for each sublevel of parameters were computed on each complete bootstrapped network in order to obtain a distribution of values. Afterwards, the sublevel-network alterations manifested in patients with AD were statistically analyzed, comparing them with the radii values of the healthy controls (HC) group. Finally **(3c)**, a classification stage was conducted in order to evaluate the potential of ANs to differentiate between HC subjects and patients with AD.

2.1. Participants

Three databases were analyzed in this study: a MEG database and two EEG databases. In the case of the MEG database, which was registered at the Hokuto Hospital (Obihiro, Japan) and at the Kumagaya General Hospital (Kumagaya, Japan), 132 participants were enrolled, divided into 55 HC individuals and 87 patients with dementia due to AD. The first EEG database, named EEG1, which comprised residents of the North of Portugal or the autonomous region of Castile and Leon (Spain), consisted of 151 participants, divided into 51 HC

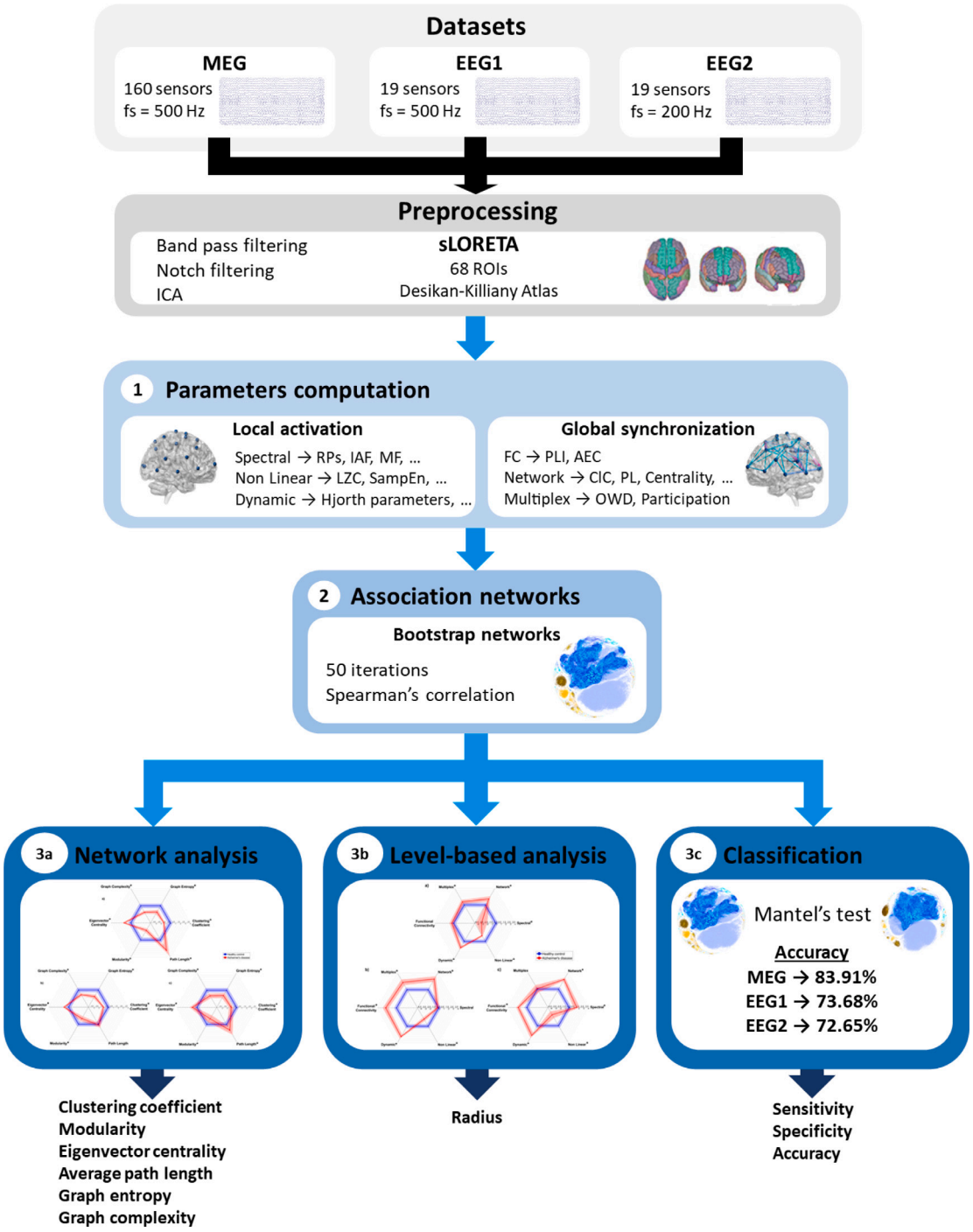

Fig. 1. Analysis-steps of the study. **(1)** Computation of the parameters that characterize the different brain activity levels of analysis: local activation (spectral, nonlinear, and dynamic features), and global synchronization (FC, frequency-dependent network parameters, and multiplex organization). **(2)** Computation of the ANs through 50 bootstrap iterations. **(3a)** and **(3b)** Global and level-based analyses, respectively, to assess the alterations that AD elicits in the neurophysiological organization of the resting-state activity. In **(3a)** a global analysis was carried out to quantify diverse network properties: segregation, integration, centrality, modularity, diversity, and complexity. In **(3b)** a level-based analysis was performed, calculating the radii of each sublevel cluster. In **(3c)** a classification stage was performed to test the capability of the methodology to discriminate between groups.

individuals and 100 patients with dementia due to AD. The second EEG database, named EEG2, which was registered at the Department of Clinical Neurophysiology of the "Río Hortega" University Hospital (Valladolid, Spain), was formed by 127 participants, divided into 45 HC individuals and 82 patients with dementia due to AD. These three databases were employed to analyze replicability not only between M/EEG recordings, but also between EEG databases (see Section 1 for further information). Patients were diagnosed following the standardized criteria of the National Institute of Aging and Alzheimer's Association (NIA-AA) [35]. If required, these examinations were complemented with additional analyses, including neuroimaging and blood samples. In addition, the cognitive and functional capabilities of the participants were assessed with the Mini-Mental State Examination (MMSE) [36] and Functional Assessment Staging (FAST) [37]. Control

Table 1
Socio-demographic and clinical data for each database. AD: Alzheimer's disease; HC: Healthy control; m: median; IQR: interquartile range; M: male; F: female; MMSE: Mini-Mental State Examination score.

MEG	Group	
	Patients with AD	HC individuals
Number of participants	87	55
Age (years) (m[IQR])	83.0[76.0, 86.0]	75.0[69.2, 78.7]
Sex (M:F)	35:52	26:29
MMSE (m[IQR])	19[14, 22]	29[28, 30]
EEG1	Group	
	Patients with AD	HC individuals
Number of participants	100	51
Age (years) (m[IQR])	82.0[76.0, 86.0]	79.0[75.0, 85.5]
Sex (M:F)	28:72	26:25
MMSE (m[IQR])	20[13, 22]	29[28, 30]
EEG2	Group	
	Patients with AD	HC individuals
Number of participants	82	45
Age (years) (m[IQR])	81.6[76.3, 83.5]	75.6[73.9, 78.6]
Sex (M:F)	34:48	14:31
MMSE (m[IQR])	21[18, 24]	29[28, 30]

groups were formed by elderly individuals with no history of neurological or psychiatric disorders. Additional inclusion and exclusion criteria were defined for patients with AD. Inclusion requirement was ages older than 65. Exclusion criteria included clinical history of neoplasia, clinical history of other neurological or psychiatric diseases, advanced dementia, recent surgery, hypercatabolic states, vascular pathology and medication that could have a tangible effect on M/EEG activity. As the participants were elderly individuals, resting-state recordings were employed. During the resting-state condition, participants were not required to perform any specific tasks, simplifying the acquisition process and ensuring a more comfortable experience [24]. Participants' clinical and socio-demographic data are summarized in Table 1. Differences in age and sex were assessed for each database, obtaining statistically significant differences in age for MEG and EEG2 databases (p-value < 0.01, Mann–Whitney U-test) and in sex for EEG1 database (p-value < 0.01, Chi-square test). To account for potential biases arising from age and sex, partial correlations were employed (see Section 2.6 for further information).

Informed consent was given by the enrolled participants, legal representatives, family or caregivers to join the study, in accordance with the recommendations of the Code of Ethics of the World Medical Association (Declaration of Helsinki). The protocol was approved by three organizations: (i) for MEG database by the Ethics Committee of Kumagaya General Hospital in Kumagaya, Japan, and Hokuto Hospital in Obihiro, Japan (097-01); (ii) for EEG1 database by the Ethics Committee of the University of Porto, Portugal (38/CEUP/2018); and (iii) for EEG2 database by the Ethics Committee of the "Río Hortega" University Hospital in Valladolid, Spain (36/2014/02).

2.2. MEG recordings and pre-processing

A MEG database was employed in this study. MEG signals consist of five minutes of resting-state brain activity recorded with a 160-channel Yokogawa Electric MEG Vision PQ1160C axial gradometers system at the Hokuto Hospital, and a 160-channel RICOH 160-1 (RICOH Co. Ltd., Tokyo, Japan) axial gradiometers system at the Kumagaya General Hospital. The acquisition sampling frequency was set at 1000 Hz and 2000 Hz, respectively. Additionally, a 200 Hz low-pass filter was applied. Subsequently, the MEG signals were downsampled to 500 Hz to match the highest sampling frequency of the EEG databases and minimize computational overhead. Head position was registered employing five fiducial markers placed on the head of each patient during the MEG recording: 40 mm above the nasion point, 10 mm in front of the tragus on each side of the head, in the left pre-auricular, and in the right pre-auricular. Participants were asked to remain calm and awake with eyes closed in a supine position during the acquisition. MEG recordings were monitored in real time for security reasons, and to prevent somnolence as well.

The signals were preprocessed according to the following steps [8, 38]: (i) artifact removal employing the SOUND algorithm [39]; (ii) notch filtering at 50 Hz to remove power-line noise; (iii) finite impulse response (FIR) filtering: a 1–70 Hz band-pass to limit the noise bandwidth, and a band-stop to erase line noise; (iv) independent component analysis (ICA) to remove artifacted components related with other biomedical signals, such as heartbeat or blinks; and (v) visual rejection of artifacted epochs.

2.3. EEG recordings and pre-processing

Two different EEG databases were used in this study. The EEG1 database was recorded using a 19-channel Nihon Kohden Neurofax JE-921A EEG system with a sampling frequency of 500 Hz, while the EEG2 database was recorded using a 19-channel XLTEK® Natus Medical EEG system with a sampling frequency of 200 Hz. In both databases, EEG activity was recorded from 19 electrodes: F3, F4, F7, F8, Fp1, Fp2, T3, T4, T5, T6, C3, C4, P3, P4, O1, O2, Fz, Cz, and Pz, following the international 10–20 system. During EEG1 database acquisition, common average reference was employed. For EEG2 database, bipolar registration was used, re-referencing those recordings to a common average reference during the preprocessing stage.

In both databases, five minutes of resting-state EEG activity were obtained. Participants were asked to remain awake and relaxed during the procedure, which was monitored in real time to avoid episodes of sleepiness. Subsequently, the signals underwent the following preprocessing steps [8,38]: (i) mean removal; (ii) notch filtering at 50 Hz to remove power-line noise; (iii) Hamming-window bandpass filter between 1 and 70 Hz to limit spectral content; (iv) independent component analysis (ICA) to remove artifacted components related with other biomedical signals, such as heartbeat or blinks; (v) segmentation into 5 s epochs; and (vi) visual inspection to remove artifacted epochs.

2.4. Source localization: sLORETA

Once the M/EEG recordings were acquired and preprocessed, source-level activity was computed employing the standardized Low-Resolution Brain Electromagnetic Tomography (sLORETA) source localization algorithm [40], in order to set a common workspace to all three databases employed in this study. sLORETA allows the computation of 3D linear solutions for the inverse problem, which permits to remove the volume conduction effects caused by the different permittivity and permeability coefficients of the brain, skull, and scalp tissues. Moreover, sLORETA restricts the solutions assuming that the correlation between neighbor neural generators is maximal, achieving spatially smoothed solutions. An identity matrix was used as noise covariance, as there were no available noise recordings. While performing sLORETA algorithm, the source-level neural generators were grouped in 68 regions of interest (ROIs) according to the Desikan-Killiany atlas, a gyrus-based schema of different brain regions corresponding to their dominant functionalities [41]. The main limitation of EEG is its spatial resolution, as the activity estimated in different ROIs could be affected by leakage from other brain regions. This effect could lead to spurious connectivity outcomes [42]. Due to the different number of sensors employed on each database (the MEG database was recorded using 160 electrodes, and both EEG databases were acquired using 19 electrodes), the Desikan-Killiany atlas with 68 ROIs was employed to obtain a good trade-off between the spatial resolution at source level and the number of sensors used by each neurophysiological technique [43–47]. This source localization analysis was performed using the Brainstorm toolbox (http://neuroimage.usc.edu/brainstorm) [48].

2.5. M/EEG analyses

Diverse signal processing techniques have been widely employed in the literature to characterize the brain activity using M/EEG recordings [29,49]. In this study, these different parameters were categorized into two main levels of analysis: (i) local activation, which measures the activation of individual brain regions [50]; and (ii) global synchronization, which allows to measure the synchronization or temporal correlation between different brain regions [21]. Likewise, these two levels of analysis were further subdivided into different sublevels. Local synchronization can be grouped in three categories: (a) spectral sublevel, which includes parameters that evaluate the spectral content of the signals; (b) nonlinear sublevel, which comprises parameters that quantify the nonlinear properties of M/EEG signals; and (c) dynamic sublevel, which covers parameters that quantify the time-varying properties of M/EEG signals. Similarly, global synchronization was divided into three categories: (a) FC sublevel, which includes connectivity parameters to quantify the synchrony or coupling between different brain regions; (b) frequency-dependent network sublevel, which encompasses parameters from graph theory to summarize the functional organization of the brain network; and (c) multiplex network organization sublevel, which consists of parameters that integrate the information from different frequency-dependent FC networks. In this study, a wide variety of parameters from the aforementioned levels and sublevels were computed to comprehensively characterize the properties of the neurophysiological activity. The calculation of these parameters was carried out using MATLAB® (R2020b version, Mathworks, Natick, MA). Additional information about the parameters involved in the study is provided in the Supplementary Material.

2.5.1. Local activation level

This level comprises different parameters that characterize the properties of each M/EEG source independently. Specifically, the local activation properties that have been analyzed in this study are:

- **Spectral sublevel**. Metrics in this sublevel parameterize the intrinsic features of the spectral content of the signal. They were computed from the normalized power spectral density (PSDn). These metrics can quantify information about the frequency rhythms (relative power, RP; median frequency, MF; individual alpha frequency, IAF; transition frequency, TF; 95% spectral edge frequency, SEF95) [51–53]; others can provide information of the spectrum variability and diversity (spectral entropy, SE; Tsallis entropy, TsE; Escort-Tsallis entropy, ETsE; Rènyi entropy, RE) [14,53–55]; and others can be used to analyze different shape-related properties of PSDn (spectral variance, skewness, and kurtosis) [17].
- **Nonlinear sublevel**. The brain exhibits nonlinear behavior due to threshold and saturation phenomena governing the dynamics of individual neurons [13]. As a result, traditional linear methods may not be sufficient to fully comprehend abnormal dynamics in M/EEG signals. Instead, nonlinear dynamical analysis techniques offer a complementary approach [50]. These nonlinear parameters provide relevant information from different perspectives, including complexity (Lempel–Ziv complexity, LZC; Higuchi's fractal dimension, HFD; Katz's fractal dimension, KFD) [14,56–60], variability (central tendency measure, CTM) [56], predictability (auto-mutual information, AMI) [52], and irregularity (approximate entropy, ApEn; sample entropy, SampEn; fuzzy entropy, FuzzyEn) [52,61,62].
- **Dynamic sublevel**. Both M/EEG signals are generated by a inherently, highly dynamic system, in which time-varying features provide useful information about the fluctuations of brain activity. These parameters can measure the variability (Hjorth's activity), diversity (Hjorth's mobility), and similarity to a pure sine wave (Hjorth's complexity) [16] of the signal, and its first and second derivatives. Besides, the different shape-related properties of the temporal distribution of the signals were computed (time variance, skewness, and kurtosis) [17].

2.5.2. Global synchronization level

This level comprises different parameters that characterize the synchronization or coupling degree between two or more brain regions. The global synchronization properties that have been analyzed in this study are listed below:

- **FC sublevel**. AD is identified as a disconnection syndrome [50]; thereby the analysis of FC alterations between neuronal population is useful to study the impairments that the disease provokes. In this study, FC analysis has been carried out in each canonical frequency band (delta: 1–4 Hz; theta: 4–8 Hz; alpha: 8–13 Hz; beta 1: 13–19 Hz; beta 2: 19–30 Hz; gamma: 30–70 Hz), obtaining a grand-average value for each pair of ROIs. Specifically, we analyzed both the phase-based (phase lag index, PLI) [63,64] and amplitude-based FC patterns (amplitude envelope correlation, AEC) [64].
- **Frequency-dependent network sublevel**. The analyzed connectivity patterns between different brain regions can be also interpreted as an estimation of the functional brain network, whose properties can be quantified using different parameters from the graph theory. These properties are useful to summarize information about node characterization (average node degree, ND; average node strength, NS; global density, D) [19,33,65], integration (characteristic path length, PL), irregularity (graph entropy, GE), segregation (clustering coefficient, ClC) [25], centrality (closeness centrality, CC; betweenness centrality, BC) [19], and *Small World* properties (*small world* index, SW) [19,66].
- **Multiplex organization sublevel**. There is evidence of diverse interactions between the neural oscillations in different frequency bands [26]. This can be also observed from frequency-dependent brain networks, in which a multilayer structure can be computed by considering the functional network at each canonical frequency band [26]. Using this approach, different multiplex properties can be computed to explore the organization of the brain network across levels for both phase- (PLI) and amplitude-based (AEC) coupling metrics. Specifically, in this study, we quantified the role of each ROI as a multiplex hub (overlapping weighted degree, OWD) and the homogeneity of the connectivity contribution of a ROI with the rest among layers (participation coefficient, P) [26].

2.6. Association networks generation

ANs are graphs that summarize the pairwise relationships between diverse variables of interest [67]. ANs are composed by nodes, which in our study are the parameters described in Section 2.5 computed in different ROIs; and edges, which quantify the existing relationships between them. To ensure participant-wise consistency, a bootstrap procedure with 50 iterations was conducted to build the correlation matrices from each database. The smaller group size (45 participants) was used to calculate the bootstrapped samples. Participants were randomly selected with uniform probability and participant repetition on each bootstrap iteration. The median value of the 50 iterations was used to generate each AN. In total, 6 ANs were obtained to characterize the neurophysiological organization (2 groups × 3 databases). The Spearman's partial correlation was calculated between each pair of M/EEG features, adjusted by sex and age due to their observed statistically significant differences (see Section 2.1 for further information). Each calculation resulted in a correlation matrix of $n \times n$ dimensions, being n the number of variables. Secondly, due to the large number of edges, only the highest absolute values of associations were kept; thereby, statistically significant absolute values of correlation equal or higher than 0.8 were retained. Afterwards, they were displayed using the *Gephi* software [68]; particularly, the Force Atlas 2 algorithm was applied, which builds embedded network layouts based on a attractor or repulsor factor driven by the node degree [69]. In this study,

the color of the nodes represents the different parameter sublevels, depicting local activation level as cold colors (spectral — grayish blue, nonlinear — dark blue, dynamic — light blue), and global synchronization level as warm colors (FC — brown, frequency-dependent network — yellow, and multiplex network organization — orange), whereas edges width and color depend on the intensity of the correlation and the variables that edge is connecting, respectively. Additionally, node width represents the weighted node degree, assigning bigger nodes to higher values of weighted node degree, and vice versa.

2.7. Network analysis

Diverse graph properties were extracted from the ANs in order to evaluate the characteristics of the whole neurophysiological organization, which was represented by the ANs, and how are they altered due to AD development [33,34]: (i) segregation (estimated by means of the clustering coefficient), that quantifies the presence of clusters with high intraconnectivity; (ii) centrality (by means of the eigenvector centrality), that measures the ability of a node to maintain the structural integrity of the network; (iii) modularity, which indicates the network ability to be divided into clusters with high intraconnectivity and low interconnectivity; (iv) integration (calculated with the characteristic path length), which is the degree of interconnection between pairs of nodes; (v) irregularity (estimated with the graph entropy), which measures the diversity of nodes weights; and (vi) complexity (computed with the graph complexity), which evaluates the ability of a graph to store meaningful information, also representing a balance between "information" and "order" [70]. Before computing these parameters, disconnected nodes were removed from each bootstrapped network, and then they were normalized by their density in order to remove the effect of different size. Finally, due to the different range of values of each graph parameter, a normalization was applied by employing the HC group from each database as reference.

2.8. Level-based evaluation

In order to assess the AD-inducing alterations to the different sublevels of parameters, a level-based evaluation was performed. Particularly, the radius, which is a metric derived from eccentricity, of each sublevel cluster was calculated. Radius is defined as the minimum eccentricity value of the entire network [71], being the eccentricity the maximum distance (*i.e.*, the maximum shortest path length) between two nodes [71]. In this regard, the radius could be a measure of integration. Thus, all sublevels of analysis were assessed in terms of integration.

2.9. Classification stage

To assess the capability of the ANs to discriminate HC subjects and patients with AD, a classification approach has been applied. This methodology is based on the Mantel's test, which allows to measure the degree of similarity between adjacency matrices [72], combined with a Leave-One-Out Cross-Validation (LOO-CV) method [73]. To fulfill this task, on each iteration, a subject is removed (from HC or AD group), and then 50 bootstrapped ANs of each group were computed, before and after adding the previously removed subject again. Afterwards, the changes in the structure of the AN are assessed using the Mantel's test, which quantifies the similarity between correlation matrices obtained for the two ANs (*i.e.*, before and after removing a given subject) [72]. Finally, once the similarity was calculated, a LOO-CV step was performed to test the robustness of the classifier.

2.10. Statistical analysis

The ANs were constructed using Spearman's partial correlation to eliminate the effects of age and sex. The graphs that show the statistically significant differences between groups in terms of distance were generated with *Gephi* (https://gephi.org/) [68].

Afterwards, as the measures did not meet parametric assumptions, Mann–Whitney U-tests were conducted to determine statistically significant differences between HC individuals and patients with AD for all the computed metrics, including graph parameters and radii. The significance threshold was set to with $\alpha = 0.05$. In order to control type I error, Bonferroni correction was performed in these pairwise comparisons. Signal processing and statistical analysis were carried out using MATLAB® (R2020b version, Mathworks, Natick, MA).

3. Results

3.1. Global analysis

The obtained ANs, which represent the neurophysiological organization of each group under study, are displayed in Fig. 2. Graph properties were computed for the bootstrap ANs in order to characterize how the distribution of these parameters is modified due to the AD, and to establish a statistical comparison between groups. A threshold of 0.8 was applied to those ANs. Fig. 3 depicts the mean and the standard deviation of the normalized parameters that represent ANs properties, obtained from MEG, EEG1, and EEG2 databases. In addition, Figure S1, provided in Supplementary Material, displays the distribution of each parameter computed for all bootstrap iterations and the three databases.

This analysis is helpful to assess how the neurophysiological organization is altered due to AD. For all databases, statistically significant differences were found in ClC, modularity, graph complexity, and graph entropy, which show lower values for patients with AD compared to HC individuals (p-values < 0.05, Mann–Whitney U-tests, Bonferroni correction). The opposite tendency is observed for eigenvector centrality, which obtains higher values for patients with AD compared to HC individuals, and statistically significant differences between groups (p-values < 0.05, Mann–Whitney U-tests, Bonferroni correction). Finally, PL is the only parameter that does not obtain statistically significant differences for all databases. As observed in Fig. 3, averaged PL shows higher values in patients with AD than in HC, but only statistically significant differences for MEG and EEG2 databases (p-values < 0.05, Mann–Whitney U-tests, Bonferroni correction). Table S1, which is available in the Supplementary Material, displays the exact p-values that have been obtained.

3.2. Level-based analysis

In order to assess how AD alters the different levels of analysis and sublevels of parameters, a level-based analysis was performed. Fig. 2 depicts that the local activation level is concentrated in a main cluster, whereas the global synchronization level is split in smaller clusters. It is shown that the general tendency for the three databases reflects higher similarity between the different sublevels of parameters of the local activation level, and higher dispersion between global synchronization parameters.

Fig. 4 shows that, for all databases, there is a statistically significant increase of the radius in the dynamic and network sublevels for patients with AD, and a statistically significant decrease in the nonlinear sublevel for patients with AD compared to HC (p-values < 0.05, Mann–Whitney U-tests, Bonferroni correction). On the other hand, the spectral sublevel shows different tendencies for each database: a significant lower radius for patients with AD in the MEG database, and the opposite tendency in the EEG2 database (p-values < 0.05, Mann–Whitney U-tests, Bonferroni correction). Finally, FC and multiplex

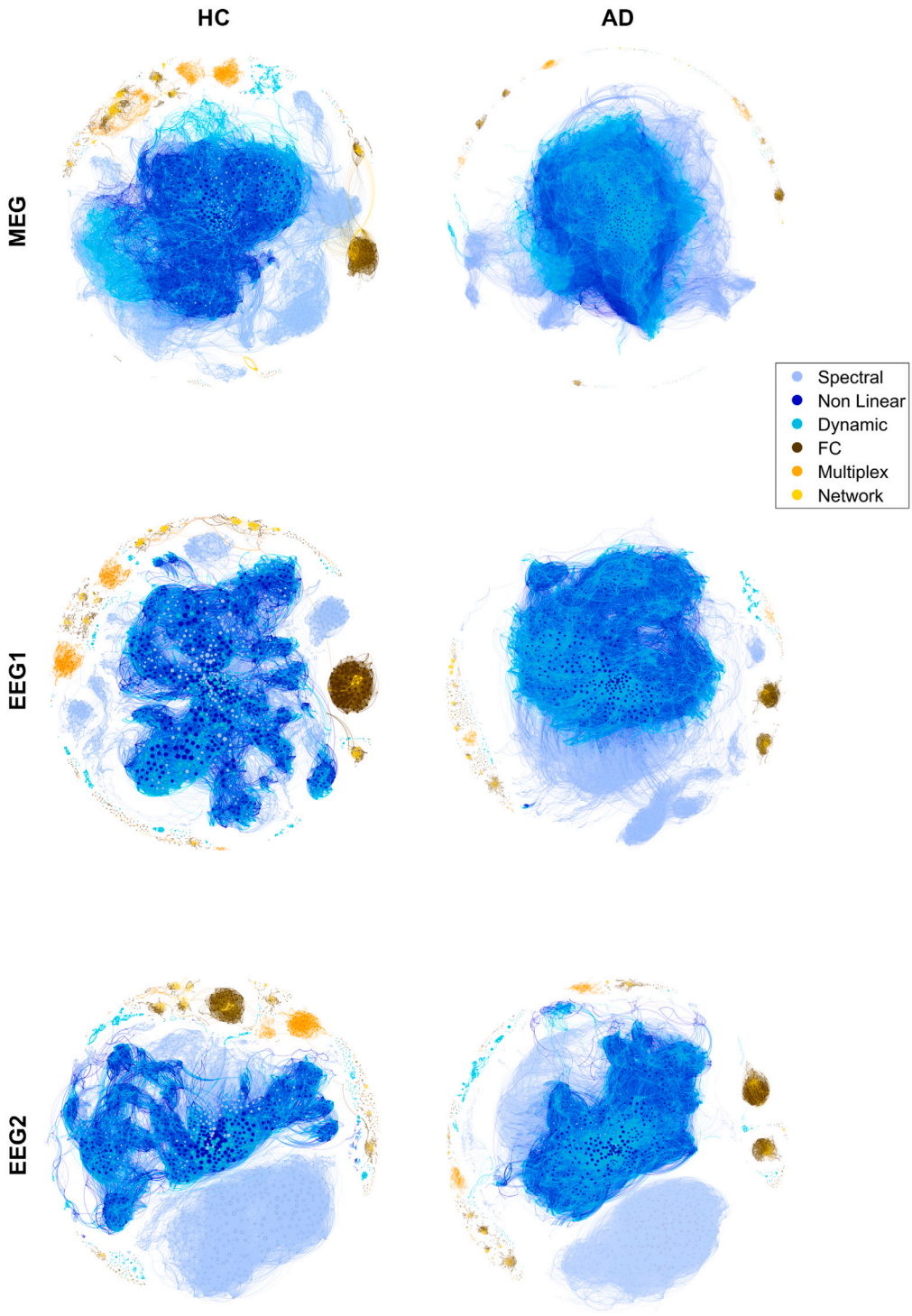

Fig. 2. Median ANs obtained for HC and AD groups on each database after bootstrapping. Cold colors represent local activation level: (i) grayish blue: Spectral sublevel; (ii) dark blue: Nonlinear sublevel; (iii) light blue: Dynamic sublevel. Warm colors depict global synchronization level: (i) brown: FC sublevel; (ii) yellow: Frequency-dependent network sublevel; (iii) orange: Multiplex organization sublevel. Node size represents the weighted node degree, depicting a larger width as the weighted node degree increases, and vice versa.

organization sublevels display the same trend for all databases, with higher radii in patients with AD compared to HC, although reflecting the former statistically significant differences in EEG databases and the latter in MEG and EEG1 databases (p-values < 0.05, Mann–Whitney U-tests, Bonferroni correction). Table S2, available in the Supplementary Material, displays the exact p-values that have been obtained.

3.3. Classification stage

Finally, a classifier was designed to discriminate between HCs and patients with AD. In this regard, sensitivity, specificity, and accuracy values were computed for all databases. For the MEG database, an accuracy of 83.91% (91.31% sensitivity, 77.63% specificity) was obtained, overcoming the accuracy values of the EEG databases (for EEG1:

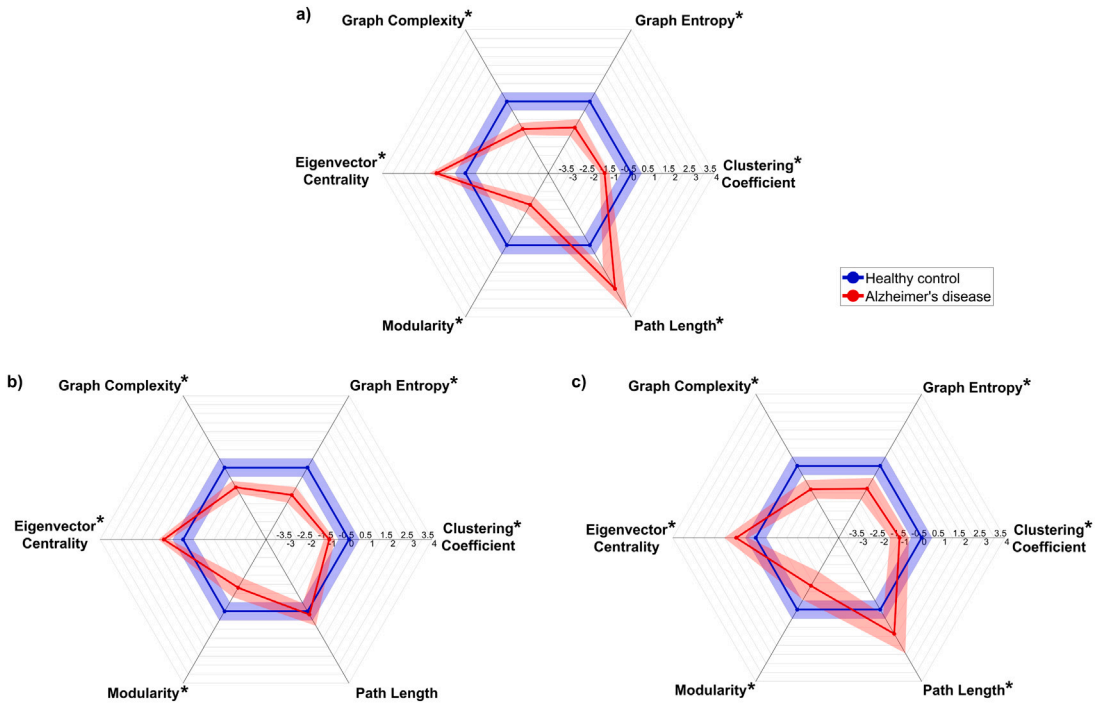

Fig. 3. Polygonal plots with the normalized values of the network parameters, where the blue line represents HC group, and the red line displays patients with AD group. (a) MEG database. (b) EEG1 database. (c) EEG2 database. Asterisks represent statistically significant differences between groups (p-value < 0.05, Mann–Whitney U-test, Bonferroni correction).

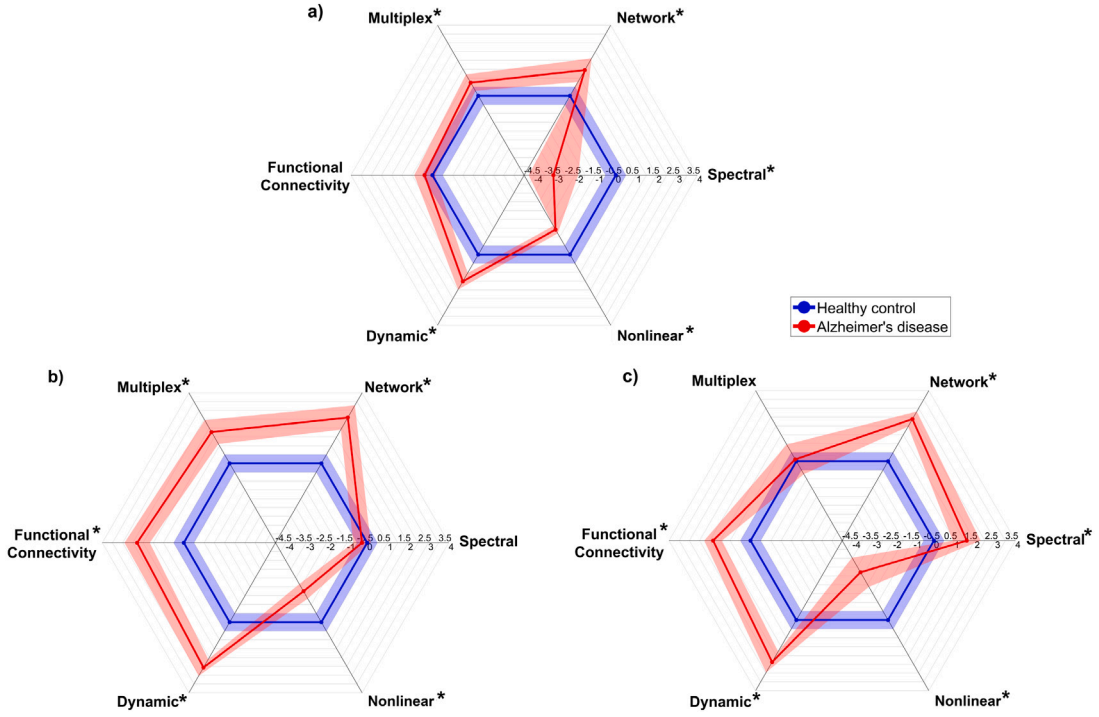

Fig. 4. Radius values for each parameter sublevel on each database. (a) MEG database. (b) EEG1 database. (c) EEG2 database. Asterisks represent statistically significant differences between groups (p-value < 0.05, Mann–Whitney U-test, Bonferroni correction).

93.28% sensitivity, 35.06% specificity, and 73.68% accuracy; for EEG2: 83.48% sensitivity, 52.91% specificity, and 72.65% accuracy).

4. Discussion

In this study, we introduced a novel methodology to explore the alterations of the neurophysiological organization in AD by analyzing the relationships between different sublevels of parameters extracted from M/EEG signals. Our results show that patients with AD exhibit alterations in neurophysiological organization at various levels of abstraction: global and level-based evaluations; when compared to HC individuals. Crucially, these results reflect a high degree of replicability, particularly for the global analysis.

4.1. Disruption of the neurophysiological organization

The ANs can be considered the map of the existing relationships that form the neurophysiological organization of the neural activity. This global representation allows for the interpretation of the brain functionality as a system characterized by different properties, such as integration, segregation, modularity, centrality, complexity, and diversity. To evaluate how these properties are altered due to AD, several graph parameters were computed from resting-state M/EEG recordings. As observed in Fig. 3, network parameters have proven useful to quantify the alterations that AD induces in the neurophysiological organization compared to HC individuals. Our results revealed that the neurophysiological organization in AD is characterized by increased PL, centrality, graph complexity, and graph entropy, as well as decreased ClC and modularity, in comparison with HC individuals. ClC and PL quantify segregation and integration, respectively, so taken together can be used to measure the small-worldness (SW). On the other hand, modularity and centrality measure the specialization capability of a network. Finally, graph complexity and graph entropy give further insight into graph diversity.

First, the ANs show a decrease in segregation and integration properties in patients with AD compared to HC individuals, represented by lower ClC and higher PL values, respectively. The ratio between ClC and PL defines the SW properties of the network [19]. Networks with high SW values are characterized by high local clustering and low average distance between nodes [74]. These characteristics correspond to neither regular nor random network configurations, but strike a balance between them. SW networks are considered to reflect optimal equilibrium in terms of local correlations and global communication in comparison to other network configurations [75]. It has been suggested that "a well-designed anatomical network" displays SW properties [19]. In line with that, we can assume that a healthy brain displays SW properties, and thus divergences in this organization could be perceived as pathological. The interpretation of divergences from maximal SW values is two-fold depending on the stochasticity, which is related with distributions of more or less random associations: ANs with increased stochasticity lead to random networks, while those with decreased stochasticity result in regular networks [50,75]. In this regard, graph entropy values are lower in the AD group than in the HC group; hence, we can infer that ANs in patients with AD show more lattice-wise regular organization. This observation could be interpreted as a reorganization of the neurophysiological organization in AD towards a less stochastic configuration. Such reorganization could be the result of a decreased presence of complex patterns due to cell damage in diverse neural populations, associated with different functions that are altered in AD [76].

Second, graph entropy and graph complexity showed decreased values in ANs for patients with AD. As mentioned beforehand, the decrease in graph entropy suggests a less uniform correlations distribution in AD. It is important to note that drawing conclusions from solely entropy values should be conducted with caution. Given that entropy values are not strictly measuring "structural richness" [77], complementary metrics such as complexity must be considered. Complexity is the ability of a system to store meaningful information, and it provides additional insights to evaluate this "structural richness" [77,78]. The relationship between entropy and complexity is a convoluted topic that nowadays is still under debate. An accepted standpoint is that highly complex systems are characterized by values of entropy that are not maximum nor minimum, but rather display intermediate values [77]. This perspective results in a relation between entropy and complexity manifested as a bell function [15,70]. For this reason, if patients with AD show decreasing values of entropy and complexity, their neurophysiological organization exhibits less diversity properties towards lower portions of the curve. Presuming that HC manifest optimal relationships configurations, healthy brain functionality might be richer in terms of information processing. Therefore, the decreased diversity and complexity observed in the neurophysiological organization of patients with AD could be identified as a pathological sign.

Third, modularity and centrality are appropriate parameters for describing network specialization. Centrality reflects the tendency of a network to contain nodes that are critical in its organization. These nodes, also called "hubs", play a key role in network resilience against disruptions [19]. On the other hand, modularity quantifies the presence of smaller functional sub-groups within a network [65]. Lower modularity in ANs of patients with AD suggests a loss of specialized groups of parameters and regions that interact in more meaningful ways than with others. This could be due to an increment of aberrant M/EEG activity elicited by damaged neural pools. Another possibility could be lack of anatomical pathways led by neural atrophy, which aligns with the "disconnection syndrome" ascription of AD [50,65]. Furthermore, centrality has been observed to increase in ANs from patients with AD. This insight is the result of an increased hub density of the network. That is, an increased number of nodes present hub properties, configuring patients with AD' ANs with star-shaped topologies. In these configurations, hub nodes are characterized by a high node degree. If these nodes were altered, the structural integrity of the network would be compromised. Thus, these networks configurations present higher vulnerability, as hub nodes are pivotal in its structural integrity [79]. From AN standpoint, this could indicate fewer parameters and/or ROIs that are much more correlated with the other parameters and/or ROIs, but also a lack of correlation between them. This lack of correlation between secondary nodes (*i.e.*, nodes with lower hub properties) leads to more vulnerable ANs, which could be associated with pathological states. Additionally, the loss of centrality can be associated with a loss of hierarchical features of the relationships between different sublevels. High centrality values, accompanied by low SW values could mean a shifting of the graph structure towards less hierarchical ANs. Noteworthy, healthy brain functional networks have been suggested to present hierarchical modular structures [80–82]. It is observed that the ANs of the patients with AD show anti-SW properties and a loss of diversity, therefore diverging from the optimal state that HC are presumed to display. Thus, the deviation that the ANs of the patients with AD show regarding those of HC reflect could be interpreted as a pattern of disruption the disease provokes. It could be also interpreted as alterations that some cognitive functions, represented as parameters and/or ROIs, display. These alterations could reflect that the "hub" nodes have to assume the functions secondary nodes lost, as a result of brain plasticity mechanisms [83].

Finally, from a level-based perspective, patients with AD ANs shows higher radius values in the global synchronization sublevels. As the radius measures the lowest maximum distance between nodes, global synchronization level presents higher distances between nodes. Hence, that increment could be interpreted as a decreased integration of the global synchronization level. These alterations could reflect not only a reduced correlation between FC, frequency-based network organization, and multiplex network organization parameters, but decreased correlations between brain regions as well. In the former case, it has been observed that there is not a solid consensus estimating those parameters; hence, different or contradictory outcomes could be obtained, which may weaken the correlation between global synchronization parameters [20]. On the other hand, the lack of correlation between brain regions could be supported by the disconnection syndrome hypothesis [50]. However, local activation sublevels do not show similar tendencies. Nonlinear sublevel displays lower radius values in patients with AD compared to HC individuals, whilst dynamic sublevel shows higher radius values in patients with AD. Of note, spectral sublevel does not show similar tendencies between databases, offering disagreeing results. Lower radius values in the spectral subgroup were observed in MEG database, which indicates higher correlations between nodes and, thus, a higher integration in the spectral parameters cluster. This insight may be due to different reasons. Firstly, it can be due

to the high signal-to-noise ratio (SNR) that MEG recordings present, providing a cleaner signal than EEG [84]. The spectral parameters could be especially affected by this issue, which might be reflected in the obtained outcomes. Secondly, the effect of the sampling frequency (500 Hz for MEG, 500 for EEG1, and 200 for EEG2 databases) could affect the spectral resolution of the techniques, which may modify the relationships between the spectral properties [85]. And thirdly, EEG2 displayed an opposite trend in its spectral cluster radius, which exhibited a significant increase compared to MEG and EEG1 databases. It turns out that the conditions that outlined the acquisition protocol that gave rise to EEG2 fitted clinical standards for diagnostic purposes. For this reason, the SNR of the EEG signals in this database is generally lower than in the recordings of MEG and EEG1 databases. Thus, the association between the presence of noise that may disturb spectral correlations and the radius in this cluster becomes apparent. This, nonetheless, highlights the usefulness of association networks, as they are able to dilute the effect of noise in the signal. This allows for establishing means of analysis that are more robust to discrepancies in acquisition conditions. Finally, the higher integration observed in the nonlinear sublevel could be a sign of more predictable and linear neural oscillations on the whole brain. Due to the increased linearity and predictability of the brain activity, it could be suggested that the dynamic sublevel become increasingly important, as they can reflect the changes of these impaired time series and differentiate between HC individuals and patients with AD [17].

4.2. Replicability between M/EEG databases

Our results reflect similar tendencies between M/EEG in the graph parameters computed on the ANs, as it can be seen in Figs. 3 and S1. The consistency of the obtained results supports the replicability of both M/EEG data. This reflects that, although these two signals present intrinsic differences, its combined use can provide a more complete understanding of the brain function [86]. Moreover, the replicability of the results obtained from M/EEG data is crucial in establishing a robust methodology for the study of brain disorders. The replication crisis in science highlights the importance of obtaining consistent and reproducible results, and the use of different neurophysiological techniques such as M/EEG can contribute to achieving this goal [30].

However, the level-based evaluation showed lower degree of replicability between databases than the global analysis. As it can be observed in Figure S2 (see Supplementary Material for further information), analyzing the stability of the neurophysiological organization from a global perspective the ANs display a high stability. In this assessment, the correlation values used to carry out the evaluation and its confidence interval do not overlap with zero, which means that the existing relationships are not due to chance. It can be suggested that the high stability, and hence the high degree of replicability, could have been achieved due to the plethora of parameters that have been included. Nevertheless, as observed in Fig. 4, even though the level-based analysis has shown its utility in distinguishing between groups, its replicability has been found to be comparatively lower than that of global analysis. This suggests that integrative approaches, like the one proposed in this study, provide smoothing on the variations that the level-based analysis would show. The sublevel metrics could display higher sensitivity to subtle analysis conditions, such as preprocessing stages or acquisition process. That could be the reason why previous studies found contradictory outcomes while assessing the same parameter [20,87]. With the use of ANs, the impact of these factors is reduced, which supports the robustness of our methodology in depicting alterations in the neurophysiological organization due to AD.

It is evident that the methodology proposed in this study has the potential to provide a more comprehensive understanding of the alterations in the neurophysiological organization of patients with AD. The results indicate that alterations in local activation parameters, specially in nonlinear and dynamic sublevels, and global synchronization measures are consistent across M/EEG databases, suggesting a shift towards a more centralized topology in patients with AD. This result may indicate that the local activation level plays a more critical role in maintaining the global stability of the neurophysiological organization in patients with AD. These findings have significant implications for our understanding of AD pathology and provide new insights into functional neural organization that may aid in the development of new approaches to characterize alterations due to AD, and differentiate pathological states from healthy cognition. Overall, the proposed methodology offers a new perspective on neural signal analysis, reflecting the potential to facilitate further progress in the field of neuroscience.

4.3. Classification performance

MEG database provides better classification outcomes than the EEG databases, which may be due to the higher signal-to-noise ratio that MEG presents, compared to EEG [84]. Other studies have tested different approaches to discriminate between HCs and patients with AD. These studies have employed different Machine Learning (ML) approaches, including Linear Discriminant Analysis (LDA), Quadratic Discriminant Analysis (QDA), and Support Vector Machine (SVM) [52,88,89], and Deep Learning (DL) architectures, such as Convolutional Neural Networks (CNN) [90]. Ruiz-Gómez et al. [52] reported sensitivity, specificity, and accuracy values ranging from 64.71% to 82.35% (LDA), 64.71% to 79.41% (QDA), and 70.59% to 82.35% (MultiLayer Perceptron, MLP). Nobukawa et al. [89] employed SVM-based classifiers to reach an accuracy value of 100% using functional connectivity features and an accuracy of 73.5% using complexity features. In another study, Miltiadous et al. [88] obtained an accuracy value of 78.5% for AD detection using decision trees. Finally, Amini et al. [90] reached an accuracy of 82.3% with CNN architectures. The classification results that have been obtained in the current work for the EEG databases are comparable to those obtained in other studies, but in some cases are lower; however, it is important to note that the purpose of the methodology proposed in the current paper, and thus the objective of our work, is not to perform classification, but to assess the alterations that AD could induce in the neurophysiological organization of the brain functional organization. On the other hand, previous studies have employed ML and DL approaches, which are powerful tools for classification.

4.4. Limitations and future research lines

Despite the fact that the present study has yielded remarkable findings, some limitations need to be mentioned.

Firstly, in this study, a plethora of parameters have been included on each sublevel of analysis (*i.e.*, spectral, nonlinear, dynamic, FC, frequency-based network organization, and multiplex network organization). These features have provided a great potential to characterize different properties of the functional neural organization. Nevertheless, they are only a sample of the great amount of other parameters that have been used in previous research works. In this regard, as a future prospect, other M/EEG parameters could be included in the analysis.

Secondly, the use of both M/EEG confers great robustness to our results, which allowed us to characterized the whole functional neural organization from its electromagnetic activity since these two signals are closely linked [7]. However, to fully characterize the global neurophysiological fingerprint of the disease, integrating additional information is of paramount importance. In that sense, the addition of information obtained from other brain imaging techniques, such as magnetic resonance image or near infrared spectroscopy, as well as sociodemographic data, clinical information, and genetics would enable the depiction of a complete image of AD by combining different perspectives into one element. This fingerprint would provide a complete

representation of the different elements involved in AD development, integrating all the information from an intuitive approach.

Finally, this novel methodology have proved useful to characterize the neurophysiological organization of the brain and to analyze its alterations due to AD. Notwithstanding, it can be also employed to provide further comprehension of the alterations that the functional neural organization may suffer due to different neurological and psychiatric pathologies.

5. Conclusions

In the present study, we proposed a novel methodology to analyze the neurophysiological organization of the functional neural organization, and characterize its alterations due to AD. The relationships between local activation and global synchronization features were assessed to that purpose. Our approach revealed that AD causes a disruption in the neurophysiological organization, showing a more centralized organization towards the local activation level. Additionally, the neurophysiological organization leads to more regular dispositions in patients with AD, characterized by more centralized and less complex topologies. These alterations could reflect more simple patterns of relationships, increasing the vulnerability of the system in AD. We believe that this work provides a new perspective to integrate the different functional neural organization properties from an integrative standpoint, and illustrates how AD alters the structure of relationships these characteristics form.

CRediT authorship contribution statement

Víctor Gutiérrez-de Pablo: Conceptualization, Data curation, Formal analysis, Investigation, Methodology, Software, Visualization, Writing – original draft. **Jesús Poza:** Conceptualization, Data curation, Funding acquisition, Methodology, Supervision, Visualization, Writing – review & editing. **Aarón Maturana-Candelas:** Data curation, Resources, Writing – review & editing. **Víctor Rodríguez-González:** Formal analysis, Writing – review & editing. **Miguel Ángel Tola-Arribas:** Data curation, Resources, Writing – review & editing. **Mónica Cano:** Data curation, Writing – review & editing. **Hideyuki Hoshi:** Data curation, Resources, Writing – review & editing. **Yoshihito Shigihara:** Data curation, Resources, Writing – review & editing. **Roberto Hornero:** Conceptualization, Funding acquisition, Writing – review & editing. **Carlos Gómez:** Conceptualization, Data curation, Funding acquisition, Methodology, Supervision, Visualization, Writing – review & editing.

Declaration of competing interest

None Declared.

Acknowledgments

This research has been developed under the grant PID2022-138286 NB-I00 funded by "Ministerio de Ciencia e Innovación/Agencia Estatal de Investigación/10.13039/501100011033/", by "ERDF A way of making Europe", and by "CIBER en Bioingeniería, Biomateriales y Nanomedicina (CIBER-BBN), Spain" through "Instituto de Salud Carlos III" co-funded with ERDF funds. Víctor Gutiérrez-de Pablo was in receipt of a PIF-UVa grant from the "University of Valladolid, Spain". Aarón Maturana-Candelas was in receipt of a PIF grant by the "Consejería de Educación de la Junta de Castilla y León, Spain".

Appendix A. Supplementary data

Supplementary material related to this article can be found online at https://doi.org/10.1016/j.cmpb.2024.108197.

References

[1] M. Vaz, S. Silvestre, Alzheimer's disease: Recent treatment strategies, Eur. J. Pharmacol. 887 (2020) 173554, http://dx.doi.org/10.1016/j.ejphar.2020.173554.
[2] Alzheimer's Disease International, World Alzheimer Report 2022 – Life after diagnosis: Navigating treatment, care and support, Tech. rep.
[3] G. Livingston, J. Huntley, A. Sommerlad, D. Ames, C. Ballard, S. Banerjee, C. Brayne, A. Burns, J. Cohen-Mansfield, C. Cooper, S.G. Costafreda, A. Dias, N. Fox, L.N. Gitlin, R. Howard, H.C. Kales, M. Kivimäki, E.B. Larson, A. Ogunniyi, V. Orgeta, K. Ritchie, K. Rockwood, E.L. Sampson, Q. Samus, L.S. Schneider, G. Selbæ k, L. Teri, N. Mukadam, Dementia prevention, intervention, and care: 2020 report of the lancet commission, Lancet 396 (2020) 413–446, http://dx.doi.org/10.1016/S0140-6736(20)30367-6.
[4] G.C. O'Neill, P. Tewarie, D. Vidaurre, L. Liuzzi, M.W. Woolrich, M.J. Brookes, Dynamics of large-scale electrophysiological networks: A technical review, NeuroImage 180 (May 2017) (2018) 559–576, http://dx.doi.org/10.1016/j.neuroimage.2017.10.003.
[5] C. Babiloni, R. Lizio, N. Marzano, P. Capotosto, A. Soricelli, A.I. Triggiani, S. Cordone, L. Gesualdo, C. Del Percio, Brain neural synchronization and functional coupling in alzheimer's disease as revealed by resting state EEG rhythms, Int. J. Psychophysiol. 103 (2016) 88–102, http://dx.doi.org/10.1016/j.ijpsycho.2015.02.008.
[6] M.X. Cohen, Where does EEG come from and what does it mean? Trends Neurosci. 40 (4) (2017) 208–218, http://dx.doi.org/10.1016/j.tins.2017.02.004.
[7] C. Pernet, M.I. Garrido, A. Gramfort, N. Maurits, C.M. Michel, E. Pang, R. Salmelin, J.M. Schoffelen, P.A. Valdes-Sosa, A. Puce, Issues and recommendations from the OHBM COBIDAS MEEG committee for reproducible EEG and MEG research, Nature Neurosci. 23 (12) (2020) 1473–1483, http://dx.doi.org/10.1038/s41593-020-00709-0.
[8] P. Núñez, J. Poza, C. Gómez, V. Rodríguez-González, A. Hillebrand, P. Tewarie, M.Á. Tola-Arribas, M. Cano, R. Hornero, Abnormal meta-state activation of dynamic brain networks across the alzheimer spectrum, NeuroImage 232 (January) (2021) 117898, http://dx.doi.org/10.1016/j.neuroimage.2021.117898.
[9] J. Gross, Magnetoencephalography in cognitive neuroscience: A primer, Neuron 104 (2) (2019) 189–204, http://dx.doi.org/10.1016/j.neuron.2019.07.001.
[10] R. Wang, J. Wang, H. Yu, X. Wei, C. Yang, B. Deng, Power spectral density and coherence analysis of alzheimer's EEG, Cogn. Neurodyn. 9 (3) (2015) 291–304, http://dx.doi.org/10.1007/s11571-014-9325-x.
[11] M.M. Engels, A. Hillebrand, W.M. Van Der Flier, C.J. Stam, P. Scheltens, E.C. Van Straaten, Slowing of hippocampal activity correlates with cognitive decline in early onset alzheimer's disease. An MEG study with virtual electrodes, Front. Hum. Neurosci. 10 (MAY2016) (2016) 1–13, http://dx.doi.org/10.3389/fnhum.2016.00238.
[12] A.H. Meghdadi, M.S. Karic, M. McConnell, G. Rupp, C. Richard, J. Hamilton, D. Salat, C. Berka, Resting state EEG biomarkers of cognitive decline associated with alzheimer's disease and mild cognitive impairment, 16, 2021,
[13] C.J. Stam, T. Montez, B.F. Jones, S.A. Rombouts, Y. Van Der Made, Y.A. Pijnenburg, P. Scheltens, Disturbed fluctuations of resting state EEG synchronization in alzheimer's disease, Clin. Neurophysiol. 116 (3) (2005) 708–715, http://dx.doi.org/10.1016/j.clinph.2004.09.022.
[14] A.H.H. Al-Nuaimi, E. Jammeh, L. Sun, E. Ifeachor, Complexity measures for quantifying changes in electroencephalogram in alzheimer's disease, Complexity 2018 (2018) 1–12, http://dx.doi.org/10.1155/2018/8915079.
[15] R. Bruña, J. Poza, C. Gómez, M. García, A. Fernández, R. Hornero, Analysis of spontaneous MEG activity in mild cognitive impairment and alzheimer's disease using spectral entropies and statistical complexity measures, J. Neural Eng. 9 (3) (2012) http://dx.doi.org/10.1088/1741-2560/9/3/036007.
[16] B. Hjorth, EEG analysis based on time domain properties, Electroencephalogr. Clin. Neurophysiol. 29 (1970) 306–310, http://dx.doi.org/10.1016/0013-4694(70)90143-4.
[17] M.S. Safi, S.M.M. Safi, Early detection of alzheimer's disease from EEG signals using hjorth parameters, Biomed. Signal Process. Control 65 (February 2020) (2021) 102338, http://dx.doi.org/10.1016/j.bspc.2020.102338.
[18] A.M. Tăuctan, E.P. Casula, M.C. Pellicciari, I. Borghi, M. Maiella, S. Bonni, M. Minei, M. Assogna, A. Palmisano, C. Smeralda, S.M. Romanella, B. Ionescu, G. Koch, E. Santarnecchi, TMS-EEG perturbation biomarkers for alzheimer's disease patients classification, Sci. Rep. 13 (1) (2023) 1–13, http://dx.doi.org/10.1038/s41598-022-22978-4.
[19] M. Rubinov, O. Sporns, Complex network measures of brain connectivity: Uses and interpretations, NeuroImage 52 (3) (2010) 1059–1069, http://dx.doi.org/10.1016/j.neuroimage.2009.10.003.
[20] C.T. Briels, D.N. Schoonhoven, C.J. Stam, H. De Waal, P. Scheltens, A.A. Gouw, Reproducibility of EEG functional connectivity in alzheimer's disease, Alzheimer's Res. Therapy 12 (1) (2020) 1–14, http://dx.doi.org/10.1186/s13195-020-00632-3.
[21] C.J. Stam, B.F. Jones, I. Manshanden, A.M. van Cappellen van Walsum, T. Montez, J.P. Verbunt, J.C. de Munck, B.W. van Dijk, H.W. Berendse, P. Scheltens, Magnetoencephalographic evaluation of resting-state functional connectivity in alzheimer's disease, NeuroImage 32 (3) (2006) 1335–1344, http://dx.doi.org/10.1016/j.neuroimage.2006.05.033.

[22] S. Afshari, M. Jalili, Directed functional networks in alzheimer's disease: Disruption of global and local connectivity measures, IEEE J. Biomed. Health Inf. 21 (4) (2017) 949–955, http://dx.doi.org/10.1109/JBHI.2016.2578954.

[23] D.F. Vecchio, D.F. Miraglia, D.F. Iberite, D.G. Lacidogna, D.V. Guglielmi, D.C. Marra, D.P. Pasqualetti, D.F.D. Tiziano, P.P.M. Rossini, Sustainable method for alzheimer dementia prediction in mild cognitive impairment: Electroencephalographic connectivity and graph theory combined with apolipoprotein e, Ann. Neurol. 84 (2) (2018) 302–314, http://dx.doi.org/10.1002/ana.25289.

[24] R. Cassani, M. Estarellas, R. San-Martin, F.J. Fraga, T.H. Falk, Systematic review on resting-state EEG for alzheimer's disease diagnosis and progression assessment, Dis. Mark. 2018 (2018) http://dx.doi.org/10.1155/2018/5174815.

[25] C.J. Stam, W. De Haan, A. Daffertshofer, B.F. Jones, I. Manshanden, A.M. Van Cappellen Van Walsum, T. Montez, J.P. Verbunt, J.C. De Munck, B.W. Van Dijk, H.W. Berendse, P. Scheltens, Graph theoretical analysis of magnetoencephalographic functional connectivity in alzheimer's disease, Brain 132 (1) (2009) 213–224, http://dx.doi.org/10.1093/brain/awn262.

[26] M. Yu, M.M. Engels, A. Hillebrand, E.C. Van Straaten, A.A. Gouw, C. Teunissen, W.M. Van Der Flier, P. Scheltens, C.J. Stam, Selective impairment of hippocampus and posterior hub areas in alzheimer's disease: An MEG-based multiplex network study, Brain 140 (5) (2017) 1466–1485, http://dx.doi.org/10.1093/brain/awx050.

[27] F. Vecchio, F. Miraglia, F. Alú, A. Orticoni, E. Judica, M. Cotelli, P.M. Rossini, Contribution of graph theory applied to EEG data analysis for alzheimer's disease versus vascular dementia diagnosis, J. Alzheimer's Dis. 82 (2) (2021) 871–879, http://dx.doi.org/10.3233/JAD-210394.

[28] J.C. McBride, X. Zhao, N.B. Munro, C.D. Smith, G.A. Jicha, L. Hively, L.S. Broster, F.A. Schmitt, R.J. Kryscio, Y. Jiang, Spectral and complexity analysis of scalp EEG characteristics for mild cognitive impairment and early alzheimer's disease, Comput. Methods Programs Biomed. 114 (2) (2014) 153–163, http://dx.doi.org/10.1016/j.cmpb.2014.01.019.

[29] J. Sun, B. Wang, Y. Niu, Y. Tan, C. Fan, N. Zhang, J. Xue, J. Wei, J. Xiang, Complexity analysis of EEG, MEG, and fMRI in mild cognitive impairment and alzheimer's disease: A review, Entropy 22 (2) (2020) 239, http://dx.doi.org/10.3390/e22020239.

[30] G. Niso, L.R. Krol, E. Combrisson, A.S. Dubarry, M.A. Elliott, C. François, Y. Héjja-Brichard, S.K. Herbst, K. Jerbi, V. Kovic, K. Lehongre, S.J. Luck, M. Mercier, J.C. Mosher, Y.G. Pavlov, A. Puce, A. Schettino, D. Schön, W. Sinnott-Armstrong, B. Somon, A.e. Šoškić, S.J. Styles, R. Tibon, M.G. Vilas, M. van Vliet, M. Chaumon, Good scientific practice in EEG and MEG research: Progress and perspectives, NeuroImage 257 (2022) http://dx.doi.org/10.1016/j.neuroimage.2022.119056.

[31] Y. Chen, A.K. Fu, N.Y. Ip, Synaptic dysfunction in alzheimer's disease: Mechanisms and therapeutic strategies, Pharmacol. Therapeut. 195 (2019) 186–198, http://dx.doi.org/10.1016/j.pharmthera.2018.11.006.

[32] D.N. Schoonhoven, C.T. Briels, A. Hillebrand, P. Scheltens, C.J. Stam, A.A. Gouw, Sensitive and reproducible MEG resting-state metrics of functional connectivity in alzheimer's disease, Alzheimer's Res. Therapy 14 (1) (2022) 1–19, http://dx.doi.org/10.1186/s13195-022-00970-4.

[33] B.M. Tijms, A.M. Wink, W. de Haan, W.M. van der Flier, C.J. Stam, P. Scheltens, F. Barkhof, Alzheimer's disease: connecting findings from graph theoretical studies of brain networks, Neurobiol. Aging 34 (8) (2013) 2023–2036, http://dx.doi.org/10.1016/j.neurobiolaging.2013.02.020.

[34] B. Ruhnau, Eigenvector-centrality-a node-centrality? Social Networks 22 (2000).

[35] G.M. McKhann, D.S. Knopman, H. Chertkow, B.T. Hyman, C.R. Jack Jr., C.H. Kawas, W.E. Klunk, W.J. Koroshetz, J.J. Manly, R. Mayeux, R.C. Mohs, J.C. Morris, M.N. Rossor, P. Scheltens, M.C. Carrillo, B. Thies, S. Weintraub, C.H. Phelps, The diagnosis of dementia due to alzheimer's disease: Recommendations from the national institute on aging- alzheimer's association workgroups on diagnostic guidelines for alzheimer's disease, Alzheimer's Dementia 7 (3) (2011) 263–269, http://dx.doi.org/10.1016/j.jalz.2011.03.005.

[36] M.F. Folstein, S.E. Folstein, P.R. McHugh, "Mini-mental state", J. Psychiatr. Res. 12 (3) (1975) 189–198, http://dx.doi.org/10.1016/0022-3956(75)90026-6.

[37] B. Reisberg, Functional assessment staging (FAST), Psychopharmacol. Bull. 24 (4) (1988) 653–659.

[38] A. Maturana-Candelas, C. Gómez, J. Poza, V. Rodríguez-González, V.G. de Pablo, A.M. Lopes, N. Pinto, R. Hornero, Influence of PICALM and CLU risk variants on beta EEG activity in alzheimer's disease patients, Sci. Rep. 11 (1) (2021) 1–11, http://dx.doi.org/10.1038/s41598-021-99589-y.

[39] T.P. Mutanen, J. Metsomaa, S. Liljander, R.J. Ilmoniemi, Automatic and robust noise suppression in EEG and MEG: The sound algorithm, NeuroImage 166 (2018) 135–151, http://dx.doi.org/10.1016/j.neuroimage.2017.10.021.

[40] R.D. Pascual-Marqui, Standardized low-resolution brain electromagnetic tomography (sLORETA): technical details., Methods Find. Exper. Clinical Pharmacol. 24 Suppl D (2002) 5–12.

[41] R.S. Desikan, F. Ségonne, B. Fischl, B.T. Quinn, B.C. Dickerson, D. Blacker, R.L. Buckner, A.M. Dale, R.P. Maguire, B.T. Hyman, M.S. Albert, R.J. Killiany, An automated labeling system for subdividing the human cerebral cortex on MRI scans into gyral based regions of interest, NeuroImage 31 (3) (2006) 968–980, http://dx.doi.org/10.1016/j.neuroimage.2006.01.021.

[42] S.R. Farahibozorg, R.N. Henson, O. Hauk, Adaptive cortical parcellations for source reconstructed EEG/MEG connectomes, NeuroImage 169 (September) (2018) 23–45, http://dx.doi.org/10.1016/j.neuroimage.2017.09.009.

[43] S. Allouch, A. Kabbara, J. Duprez, M. Khalil, J. Modolo, M. Hassan, Effect of channel density, inverse solutions and connectivity measures on EEG resting-state networks reconstruction: A simulation study, NeuroImage 271 (2023) 120006, http://dx.doi.org/10.1016/j.neuroimage.2023.120006.

[44] X. Lin, W. Kong, J. Li, X. Shao, C. Jiang, R. Yu, X. Li, B. Hu, Aberrant static and dynamic functional brain network in depression based on EEG source localization, IEEE/ACM Trans. Comput. Biol. Bioinform. 20 (3) (2023) 1876–1889, http://dx.doi.org/10.1109/TCBB.2022.3222592.

[45] M.A. Lopes, L. Junges, L. Tait, J.R. Terry, E. Abela, M.P. Richardson, M. Goodfellow, Computational modelling in source space from scalp EEG to inform presurgical evaluation of epilepsy, Clin. Neurophysiol. 131 (1) (2020) 225–234, http://dx.doi.org/10.1016/j.clinph.2019.10.027.

[46] P. Zhou, Q. Wu, L. Zhan, Z. Guo, C. Wang, S. Wang, Q. Yang, J. Lin, F. Zhang, L. Liu, D. Lin, W. Fu, X. Wu, Alpha peak activity in resting-state EEG is associated with depressive score, Front. Neurosci. 17 (2023) 1–9, http://dx.doi.org/10.3389/fnins.2023.1057908.

[47] V. Rodríguez-González, C. Gómez, Y. Shigihara, H. Hoshi, M. Revilla-Vallejo, R. Hornero, J. Poza, Consistency of local activation parameters at sensor- and source-level in neural signals, J. Neural Eng. 17 (5) (2020) http://dx.doi.org/10.1088/1741-2552/abb582.

[48] F. Tadel, S. Baillet, J.C. Mosher, D. Pantazis, R.M. Leahy, Brainstorm: A user-friendly application for MEG/EEG analysis, Comput. Intell. Neurosci. 2011 (2011) http://dx.doi.org/10.1155/2011/879716.

[49] F. Vecchio, C. Babiloni, R. Lizio, F. De Vico Fallani, K. Blinowska, G. Verrienti, G. Frisoni, P.M. Rossini, Resting state cortical EEG rhythms in alzheimer's disease: Toward eeg markers for clinical applications: A review, first ed., Supplements To Clinical Neurophysiology, vol. 62, Elsevier B.V., 2013, pp. 223–236, http://dx.doi.org/10.1016/B978-0-7020-5307-8.00015-6.

[50] C. Stam, E. van Straaten, The organization of physiological brain networks, Clin. Neurophysiol. 123 (6) (2012) 1067–1087, http://dx.doi.org/10.1016/j.clinph.2012.01.011.

[51] J. Poza, C. Gómez, A. Bachiller, R. Hornero, Spectral and non-linear analyses of spontaneous magnetoencephalographic activity in alzheimer's disease, J. Healthc. Eng. 3 (2) (2012) 299–322.

[52] S.J. Ruiz-Gómez, C. Gómez, J. Poza, G.C. Gutiérrez-Tobal, M.A. Tola-Arribas, M. Cano, R. Hornero, Automated multiclass classification of spontaneous EEG activity in alzheimer's disease and mild cognitive impairment, Entropy 20 (1) (2018) 1–15, http://dx.doi.org/10.3390/e20010035.

[53] V. Rodríguez-González, C. Gómez, H. Hoshi, Y. Shigihara, R. Hornero, J. Poza, Exploring the interactions between neurophysiology and cognitive and behavioral changes induced by a non-pharmacological treatment: A network approach, Front. Aging Neurosci. 13 (July) (2021) 1–15, http://dx.doi.org/10.3389/fnagi.2021.696174.

[54] J. Poza, R. Hornero, J. Escudero, A. Fernández, C.I. Sánchez, Regional analysis of spontaneous MEG rhythms in patients with alzheimer's disease using spectral entropies, Ann. Biomed. Eng. 36 (1) (2008) 141–152, http://dx.doi.org/10.1007/s10439-007-9402-y.

[55] R.P. Di Sisto, S. Martínez, R.B. Orellana, A.R. Plastino, A. Plastino, General thermostatistical formalisms, invariance under uniform spectrum translations, and tsallis q-additivity, Phys. A 265 (3) (1999) 590–613, http://dx.doi.org/10.1016/S0378-4371(98)00561-5.

[56] D. Abásolo, R. Hornero, C. Gómez, M. García, M. López, Analysis of EEG background activity in alzheimer's disease patients with lempel-ziv complexity and central tendency measure, Med. Eng. Phys. 28 (4) (2006) 315–322, http://dx.doi.org/10.1016/j.medengphy.2005.07.004.

[57] T. Higuchi, Approach to an irregular time series on the basis of the fractal theory, Physica D 31 (1988) 277–283.

[58] C. Gómez, Á. Mediavilla, R. Hornero, D. Abásolo, A. Fernández, Use of the Higuchi's fractal dimension for the analysis of MEG recordings from alzheimer's disease patients, Med. Eng. Phys. 31 (3) (2009) 306–313, http://dx.doi.org/10.1016/j.medengphy.2008.06.010.

[59] B.S. Raghavendra, D. Narayana Dutt, A note on fractal dimensions of biomedical waveforms, Comput. Biol. Med. 39 (11) (2009) 1006–1012, http://dx.doi.org/10.1016/j.compbiomed.2009.08.001.

[60] M.J. Katz, Fractals and the analysis of waveforms, Comput. Biol. Med. 18 (3) (1988) 145–156, http://dx.doi.org/10.1016/0010-4825(88)90041-8.

[61] R. Espinosa, J. Talero, A. Weinstein, Effects of tau and sampling frequency on the regularity analysis of ecg and eeg signals using apen and sampen entropy estimators, Entropy 22 (11) (2020) 1–14, http://dx.doi.org/10.3390/e22111298.

[62] J. Monge, C. Gómez, J. Poza, A. Fernández, J. Quintero, R. Hornero, MEG analysis of neural dynamics in attention-deficit/hyperactivity disorder with fuzzy entropy, Med. Eng. Phys. 37 (4) (2015) 416–423, http://dx.doi.org/10.1016/j.medengphy.2015.02.006.

[63] C.J. Stam, G. Nolte, A. Daffertshofer, Phase lag index: Assessment of functional connectivity from multi channel EEG and MEG with diminished bias from common sources, Hum. Brain Mapp. 28 (11) (2007) 1178–1193, http://dx.doi.org/10.1002/hbm.20346.

[64] P. Núñez, J. Poza, C. Gómez, V. Rodríguez-González, A. Hillebrand, M.A. Tola-Arribas, M. Cano, R. Hornero, Characterizing the fluctuations of dynamic resting-state electrophysiological functional connectivity: Reduced neuronal coupling variability in mild cognitive impairment and dementia due to alzheimer's disease, J. Neural Eng. 16 (5) (2019) http://dx.doi.org/10.1088/1741-2552/ab234b.

[65] W. De Haan, W.M. Van der Flier, T. Koene, L.L. Smits, P. Scheltens, C.J. Stam, Disrupted modular brain dynamics reflect cognitive dysfunction in alzheimer's disease, NeuroImage 59 (4) (2012) 3085–3093, http://dx.doi.org/10.1016/j.neuroimage.2011.11.055.

[66] F. Vecchio, F. Miraglia, F. Piludu, G. Granata, R. Romanello, M. Caulo, V. Onofrj, P. Bramanti, C. Colosimo, P.M. Rossini, "Small world" architecture in brain connectivity and hippocampal volume in alzheimer's disease: a study via graph theory from EEG data, Brain Imaging Behav. 11 (2) (2017) 473–485, http://dx.doi.org/10.1007/s11682-016-9528-3.

[67] D. Borsboom, A.O. Cramer, V.D. Schmittmann, S. Epskamp, L.J. Waldorp, The small world of psychopathology, PLoS ONE 6 (11) (2011) http://dx.doi.org/10.1371/journal.pone.0027407.

[68] M. Bastian, S. Heymann, M. Jacomy, Gephi: An Open Source Software for Exploring and Manipulating Networks Visualization and Exploration of Large Graphs, Tech. rep, 2009, pp. 361–362, URL www.aaai.org.

[69] M. Jacomy, T. Venturini, S. Heymann, M. Bastian, ForceAtlas2, a continuous graph layout algorithm for handy network visualization designed for the gephi software, PLoS ONE 9 (6) (2014) 1–12, http://dx.doi.org/10.1371/journal.pone.0098679.

[70] J. Gomez-Pilar, J. Poza, A. Bachiller, C. Gómez, P. Núñez, A. Lubeiro, V. Molina, R. Hornero, Quantification of graph complexity based on the edge weight distribution balance: Application to brain networks, Int. J. Neural Syst. 28 (1) (2018) 1–19, http://dx.doi.org/10.1142/S0129065717500320.

[71] R.A. Gutierrez Nuno, C.H.R. Chung, K. Maharatna, Hardware architecture for real-time EEG-based functional brain connectivity parameter extraction, J. Neural Eng. 18 (3) (2021) http://dx.doi.org/10.1088/1741-2552/abd462.

[72] M. Saggar, S.M. Hosseini, J.L. Bruno, E.M. Quintin, M.M. Raman, S.R. Kesler, A.L. Reiss, Estimating individual contribution from group-based structural correlation networks, NeuroImage 120 (2015) 274–284, http://dx.doi.org/10.1016/j.neuroimage.2015.07.006.

[73] T.T. Wong, Performance evaluation of classification algorithms by k-fold and leave-one-out cross validation, Pattern Recognit. 48 (9) (2015) 2839–2846, http://dx.doi.org/10.1016/j.patcog.2015.03.009.

[74] F. Miraglia, F. Vecchio, C. Pappalettera, L. Nucci, M. Cotelli, E. Judica, F. Ferreri, P.M. Rossini, Brain connectivity and graph theory analysis in alzheimer's and parkinson's disease: The contribution of electrophysiological techniques, Brain Sci. 12 (3) (2022) http://dx.doi.org/10.3390/brainsci12030402.

[75] X. Liao, A.V. Vasilakos, Y. He, Small-world human brain networks: Perspectives and challenges, Neuroscience and Biobehavioral Reviews 77 (2017) 286–300, http://dx.doi.org/10.1016/j.neubiorev.2017.03.018.

[76] L. Stefanovski, P. Triebkorn, A. Spiegler, M.A. Diaz-Cortes, A. Solodkin, V. Jirsa, A.R. McIntosh, P. Ritter, Linking molecular pathways and large-scale computational modeling to assess candidate disease mechanisms and pharmacodynamics in alzheimer's disease, Fron. Comput. Neurosci. 13 (2019) http://dx.doi.org/10.3389/fncom.2019.00054.

[77] M. Costa, A.L. Goldberger, C.K. Peng, Multiscale entropy analysis of biological signals, Phys. Rev. E 71 (2) (2005) http://dx.doi.org/10.1103/PhysRevE.71.021906.

[78] L.T. Trujillo, C.T. Stanfield, R.D. Vela, The effect of electroencephalogram (EEG) reference choice on information-theoretic measures of the complexity and integration of eeg signals, Front. Neurosci. 11 (JUL) (2017) 1–22, http://dx.doi.org/10.3389/fnins.2017.00425.

[79] M.P. van den Heuvel, O. Sporns, Network hubs in the human brain, Trends Cogn. Sci. 17 (12) (2013) 683–696, http://dx.doi.org/10.1016/j.tics.2013.09.012.

[80] O. Sporns, Structure and function of complex brain networks, Dialogues Clin. Neurosci. 15 (3) (2013) 247–262, http://dx.doi.org/10.31887/dcns.2013.15.3/osporns.

[81] C.J. Stam, B.F. Jones, G. Nolte, M. Breakspear, P. Scheltens, Small-world networks and functional connectivity in alzheimer's disease, Cerebral Cortex 17 (1) (2007) 92–99, http://dx.doi.org/10.1093/cercor/bhj127.

[82] S.J. Wang, C.C. Hilgetag, C. Zhou, Sustained activity in hierarchical modular neural networks: self-organized criticality and oscillations, Front. Comput. Neurosci. 5 (2011) http://dx.doi.org/10.3389/fncom.2011.00030.

[83] N. Sharma, J. Classen, L.G. Cohen, Neural plasticity and its contribution to functional recovery, in: Handbook of Clinical Neurology, vol. 110, Elsevier B.V., 2013, pp. 3–12, http://dx.doi.org/10.1016/B978-0-444-52901-5.00001-0.

[84] A.L. Fred, S.N. Kumar, A.K. Haridhas, S. Ghosh, H.P. Bhuvana, W.K.J. Sim, V. Vimalan, F.A.S. Givo, V. Jousmäki, P. Padmanabhan, B. Gulyás, A brief introduction to magnetoencephalography (MEG) and its clinical applications, Brain Sci. 12 (6) (2022) http://dx.doi.org/10.3390/brainsci12060788.

[85] D.-W. Kim, C.-H. Im, Computational EEG analysis, in: C.-H. Im (Ed.), in: Biological and Medical Physics, Biomedical Engineering, Springer Singapore, Singapore, 2018, pp. 35–53, http://dx.doi.org/10.1007/978-981-13-0908-3.

[86] S. Rampp, H. Stefan, On the opposition of EEG and MEG, Clin. Neurophysiol. 118 (8) (2007) 1658–1659, http://dx.doi.org/10.1016/j.clinph.2007.04.021.

[87] T. Takahashi, Complexity of spontaneous brain activity in mental disorders, Progr. Neuro-Psychopharmacol. Biol. Psychiatr. 45 (2013) 258–266, http://dx.doi.org/10.1016/j.pnpbp.2012.05.001.

[88] A. Miltiadous, K.D. Tzimourta, N. Giannakeas, M.G. Tsipouras, T. Afrantou, P. Ioannidis, A.T. Tzallas, Alzheimer's disease and frontotemporal dementia: A robust classification method of eeg signals and a comparison of validation methods, Diagnostics 11 (8) (2021) http://dx.doi.org/10.3390/diagnostics11081437.

[89] S. Nobukawa, T. Yamanishi, S. Kasakawa, H. Nishimura, M. Kikuchi, T. Takahashi, Classification methods based on complexity and synchronization of electroencephalography signals in alzheimer's disease, Front. Psychiatry 11 (2020) 255, http://dx.doi.org/10.3389/fpsyt.2020.00255.

[90] M. Amini, M.M. Pedram, A.R. Moradi, M. Ouchani, Diagnosis of alzheimer's disease by time-dependent power spectrum descriptors and convolutional neural network using EEG signal, Comput. Math. Methods Med. 2021 (2021) http://dx.doi.org/10.1155/2021/5511922.